Technical Sciences, 2020, 23(3), 253–262

UNIWERSYTET WARMIŃSKO-MAZURSKI W OLSZTYNIE

Quarterly peer-reviewed scientific journal
ISSN 1505-4675
e-ISSN 2083-4527
TECHNICAL SCIENCES
Homepage: www.uwm.edu.pl/techsci/

DOI: https://doi.org/10.31648/ts.6051

INFLUENCE OF PLASTIC DEFORMATION ON THE ELECTROCHEMICAL PROPERTIES OF X5CRNI18-10 STEEL

Wojciech Rejmer

ORCID: 0000-0002-1955-1553
Faculty of Technical Sciences
University of Warmia and Mazury in Olsztyn

Received 4 November 2020, accepted 9 December 2020, available online 9 December 2020.

K e y w o r d s: corrosion, electrochemistry, stainless steel, impendence spectroscopy, Tafel plots.

A b s t r a c t

The purpose of this study was to determine the effect of plastic deformation on the electrochemical properties of X5CrNi18-10 steel. The tested material belongs to the group of stainless steels with low carbon content, and it is used in many industries due to its high corrosion resistance. In most applications of the tested material, it is formed into complicated shapes and exposed to aggressive environments. Examples include the applications in medicine (implants) as well as in civil engineering and nuclear power plants. Different effects of deformation on anti-corrosion properties have been described in the literature. Samples with 5 different deformations were obtained in the present experiment. Electrochemical direct electrical current and alternating electrical current tests were performed for the obtained materials. The tests were carried out in a 1 molar sodium chloride solution. The study revealed an increase in the corrosion resistance of samples with increasing strain in the tested strain ranges.

Correspondence: Wojciech Rejmer, Katedra Technologii Materiałów i Maszyn, Wydział Nauk Technicznych, Uniwersytet Warmińsko-Mazurski, ul. Oczapowskiego 11,10-719 Olsztyn, e-mail: wojciech.rejmer@uwm.edu.pl

Introduction

Steel 1.4301 belongs to the group of corrosion-resistant steels (EN 10088-1:2014), and it has a wide range of applications. In the automotive industry, it is used, among others, as a construction material for the production of exhaust systems, catalyst and turbocharger housings, fuel tanks, truck and bus chassis, external and internal decorative elements, suspension elements, safety cages and road tankers. Various types of stainless steel are widely used due to their corrosion resistance and the possibility of producing complex and visually attractive shapes (KUŁAKOWSKI, ROKOSZ 2017) Stainless steel is also used in the production of cookware. It is estimated that around 43% of kitchen utensils are made of stainless steel (BERNSTEIN 1977, SANTONEN et al. 2010). Most of the stainless steel used in cookware contains approximately 18% chromium, which ensures optimal corrosion resistance. Apart from chromium, it also contains nickel in the amount of 8-10% (BASSIONI et al. 2015). Stainless steel is also widely used in construction. The most popular applications include the construction of glazed roofs and facades, as well as elevators and escalators. It is used for the construction of barriers and balustrades (WCIŚLIK 2017). Austenitic stainless steels are also used in medicine. They are often used in the production of orthopedic implants due to their properties, including the resistance to corrosion and fatigue, as well as high resistance to fracture. These properties are important in the selection and modification of materials for biomedical applications (RYAN et al. 2006, ALVAREZ et al. 2008). Nuclear power generation is yet another branch of industry where stainless steels are used. The construction materials for nuclear power plants should preserve the integrity of fuel rods and prevent the release of radioactive materials from the fuel into the coolant. The materials are also exposed to aggressive environments. The aggressiveness of the environment is caused by the velocity of a neutron flux combined with a high temperature. Neutron radiation causes the displacement of atoms in the nodes of a crystal lattice (*Stress Corrosion Cracking…* 2011). The above leads to void swelling, phase instability and creep that increases with the intensity of neutron radiation. To meet these conditions, the chemical composition/microstructure of stainless steels must be changed, for example by introducing smaller amounts of alloying elements such as Ti, Si and P. Recent research into the use of stainless steels as lining for nuclear fuel rods and fuel assembly components has shown that yttrium and oxide precipitates act as stable obstacles to the movement of atoms, and help block radiation. Stainless steels have also been used as a replacement for copper alloys in tube bundles for feedwater heaters. Products made from copper alloys cause galvanic corrosion, thus disturbing heat transfer (VENKATRAMAN 2013). Austenitic steels are characterized by high corrosion resistance in acidic environments, which, however, changes in response to plastic deformation. Samples deformed by cold rolling have lower corrosion resistance than non-deformed samples. Corrosion

resistance changes in environments rich in chloride ions, which cause pitting corrosion (FREIREA et al. 2011). It can be concluded that plastic deformation produced in a cold environment and at high speeds leads to the formation of local micro-cells (RUTKOWSKA-GORCZYCA et al. 2009). An increase in corrosion resistance was observed when crushing samples of AISI 321 steel to the level of 0.86. The steel used in the study had a crystallographic system of regular face-centered unit cells. Additionally, samples of different morphology were obtained by heat treatment. A decrease in corrosion resistance resulting from deformation was observed only in samples with the smallest grain sizes. Deformed samples with larger grain sizes were characterized by higher corrosion resistance. It appears that this effect is caused by the development of austenite crystallographic planes, which reduces the influence of martensitic phase formation (TIAMIYU 2019). In the tests that revealed an increase in corrosion potential, the applied deformations were single-folded, and the tests were carried out at a constant strain rate. A decrease in corrosion potential was observed for small plastic deformations in the compression cycles, leading to an increase in the hardness of stainless steel. In addition, several rolling cycles (strains greater than 0.2) were required to achieve higher levels of deformation in the rolling process. The electrochemical parameters of the analyzed samples may be influenced by the extent of deformation and the related changes in the material's structure. A breaking test was performed to examine the electrochemical and structural parameters of AISI 304 steel within the ranges of elastic and plastic strains. Comprehensive research, including electrochemical and structural tests, demonstrated that the type of deformation exerted varied effects on the electrochemical parameters of the tested material. According to research, elastic deformations do not affect the material's susceptibility to corrosion. Plastic deformations caused a significant decrease in corrosion potential. The tests were carried out during stretching. The decrease in corrosion potential during deformation was attributed to the formation of cracks in the passive oxide layer. The distortion of the layer structure probably resulted in the formation of new active surfaces enabling faster electrochemical processes to take place (NAZAROV et al. 2019). The aim of the present study was to determine the influence of plastic deformation in the tensile cycle on the electrochemical properties of X5CrNi18-10 steel (1.4301 or AISI 304). The tests were carried out 48 h after grinding the sample in order to enable the formation of an oxide layer.

Materials and Methods

Samples of X5CrNi18-10 steel used in the experiment are presented in Figure 1. The samples were cut out from a 5 mm thick metal sheet with the use of the ZAP BP09d electro-erosive cutter.

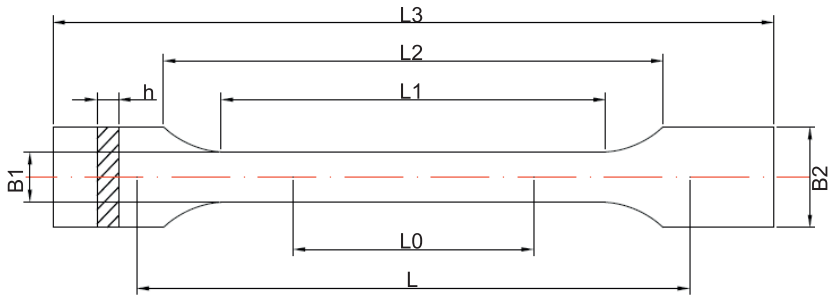

Fig. 1. Sample shapes (description in the text)

The dimensions of the samples were as follows: L0 = 30 mm, L1 = 45 mm, L2 = 60 mm, L3 =125 mm, b1 = 5 mm, b2 = 10 mm, h = 5 mm. The tensile tests were performed in accordance with Standard PN-EN ISO 6892-1. The samples were stretched at a speed of 2.5 mm/min on the Tira Test 27100 testing machine. The following deformations were obtained: 0.07; 0.12; 0.16; 0.20; 0.23. Three samples were prepared for each level of deformation. In addition, three samples were left undistorted. The samples were ground on a laboratory grinder with the use of sandpaper graded from 200 to 800 to the resulting roughness Ra of 0.4 to 0.5 μm. The test samples were left in the desiccator for 48 h and then their roughness was measured again. The samples were cleansed with acetone and placed in an electrochemical vessel (Fig. 2). The necking of the samples was the place isolated within the electrochemical unit with the use of a 5 mm diameter o-ring. Therefore, electrochemical data were obtained for the area of 19.6 mm^2.

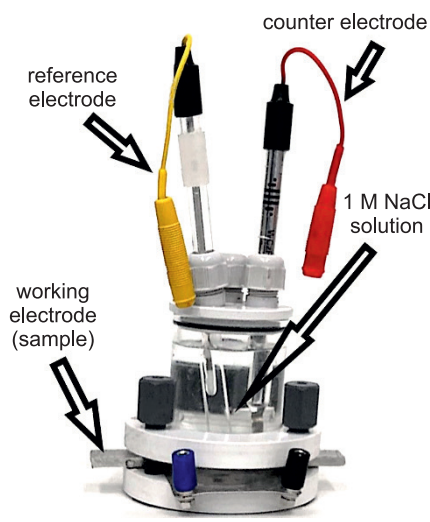

Fig. 2 . Electrochemical vessel

A 1 M NaCl solution was poured into the electrochemical vessel with the sample attached, which allows for linear changes in the conductivity of the solution without the involvement of processes related to changes in the ion activity coefficient. A silver chloride electrode as the reference electrode and a platinum electrode as the counter electrode were placed in the vessel. The Lugin capillary was placed on the reference electrode and positioned 0.5 mm above the sample. The electrodes and the sample were connected to an electrochemical unit – ATLAS 1131 EU&IA by Atlas-Solich. The system was then stabilized to steady-state potential for 6 h. The LPR was measured by lowering the potential of the working electrode by 50 mV below the stationary potential, and then increasing the potential to 50 mV above the stationary potential. Changes in the potential occurred at a rate of 1 mV/s. Impedance spectroscopy was carried out using the amplitude of potential changes of 50 mV. The measurements were performed in the frequency range of alternating current of 100 kHz to 1 mHz, using the AtlasCorr program, and the results of the analysis were processed using the AtlasLab program.

Results

The values of corrosion potential and polarization current density were obtained from the Tafel curves. An exemplary plot of the dependence of the sample potential on the logarithm of the absolute value of polarization current density determined for an undistorted sample is shown in Figure 3. Figure 4 shows the dependence of corrosion potential on the extent of plastic deformation.

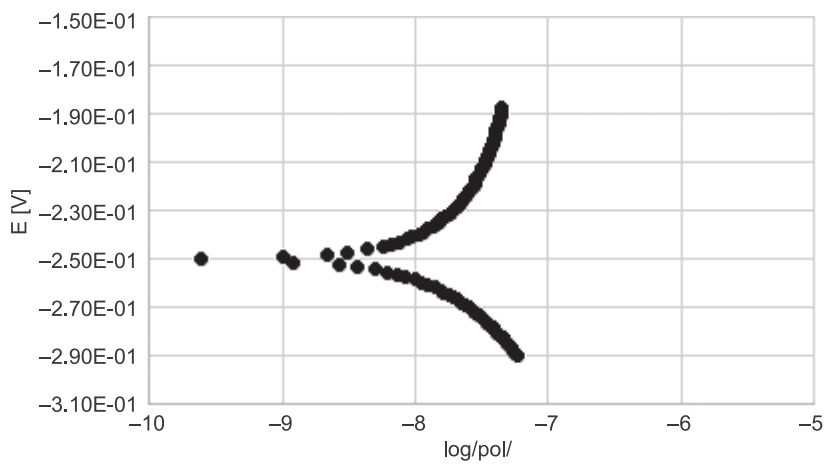

Fig. 3. The dependence of the sample potential on the logarithm of the absolute value of polarization current density determined for an undistorted sample

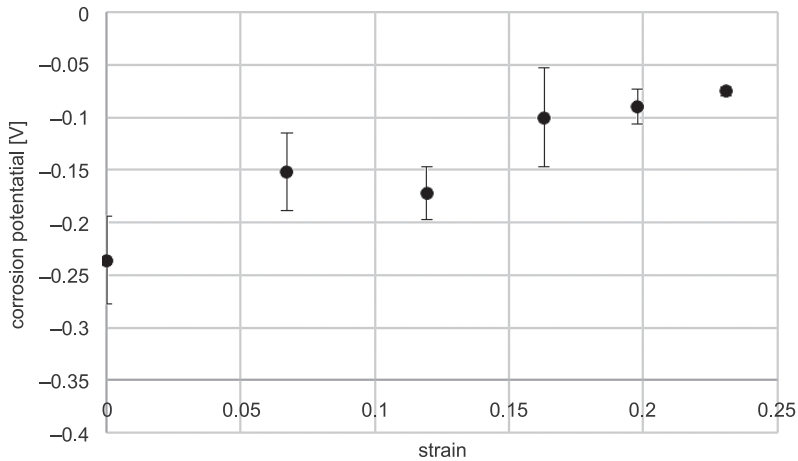

Fig. 4. The dependence of corrosion potential on plastic deformation

In the tested material, the value of corrosion potential measured against the silver chloride electrode increased proportionally to deformation. The measured values ranged from – 0.24 to – 0.075 V. The values of corrosion potential increased with increasing deformation. The only exception was the sample with a deformation value of 0.12. The remaining samples differed significantly from the non-deformed sample. A comparison of samples with deformation of 0.07 and materials with deformations of 0.2 and 0.23 revealed a significant increase in potential. Corrosion potential is a measure of the energy required for the electrochemical oxidation process to occur. The higher the potential value, the greater the material's resistance. In the analyzed specimens, deformation contributed to an increase in corrosion resistance in the test solution.

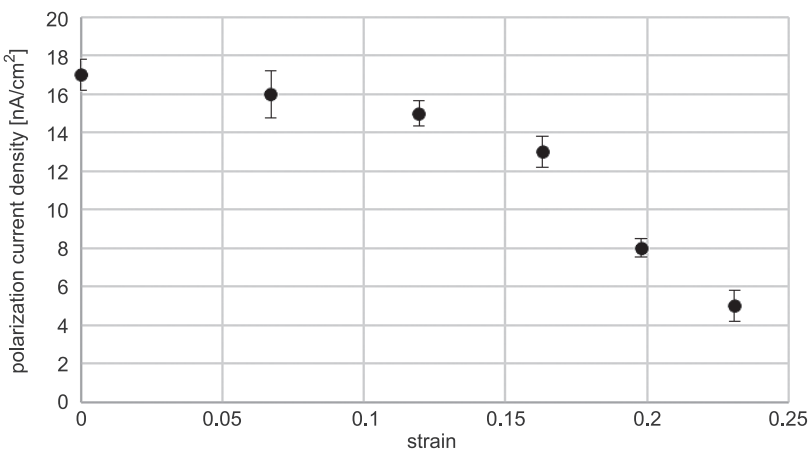

Fig. 5. The dependence of corrosion current density on the plastic deformation of samples

Another parameter determined based on an analysis of Tafel curves was corrosion current density. The values of corrosion current density for materials with specific deformations are shown in Figure 5.

Corrosion current density is inversely proportional to deformation. The highest value of crrosion current density was noted for the non-deformed sample (17 nA/cm^2). The lowest value of corrosion current density was observed for the sample with a strain of 0.23. The value of corrosion current density for the most deformed sample was 5 nA/cm^2. Current density decreased considerably after exceeding the deformation value of 0.16. The measured current densities for strains greater than 0.12 differ significantly from those determined for the undistorted sample. It should be noted that corrosion current densities were low in all cases, and remained within the nanoampere limits. The greater the value of current density, the greater the exchange of electrons on a given surface. In the tested samples, the number of oxidation reactions decreased with increasing strain.

In the next step, deformed samples were tested to determine their behavior in response to alternating current, using the EIS method. The impedance spectra in the form of Nyquist plots are presented in Figure 6.

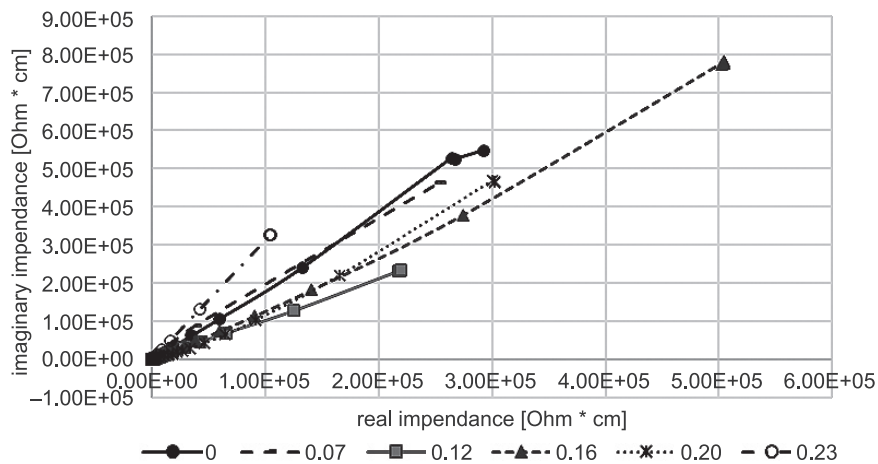

Fig 6. Impedance spectra of deformed samples

The Nyquist plots for all tested samples have the same shape of straight lines, which means that the equivalent circuit that best approximates the tested sample is a series connection of a resistor and a variable phase element (Fig. 7).

Fig 7. Equivalent circuit used in the tests

The above implies that no new chemical substances appear on the tested surfaces as a result of deformation, which makes it possible to meet the condition of the low invasiveness of the test with regard to the material's structure. It can be concluded that only the quantitative ratio of the substances already present on the material's surface changes in response to deformation. The highest real impedance was determined in samples with a deformation value of 0.16, and the lowest real impedance was noted in the most deformed samples. The second highest corrosion resistance was noted in non-deformed samples and samples with a deformation value of 0.2. The lowest values of real impedance were observed in the most deformed samples. By analyzing the slope of the curve relative to the axis of real impedance, we can assess the extent to which a given surface is covered with a non-conductive layer. In the present case, metal oxides constitute the non-conductive element. The sample that is most similar to an ideal capacitor and thus has the largest amount of metal on the surface is probably the most deformed sample. The slope of the curve in the direction of the X-axis increases with the extent of deformation up to the level of 0.12. The subsequent curves represent Nyquist plots further away from the X-axis. It can be assumed that the percentage of surface covered with oxides decreases with increasing deformation.

Discussion

The deformation of samples made of X5CrNi18-10 steel increases the corrosion resistance of the material within the range of the tested deformations, provided that only DC tests are taken into account. Corrosion potential, which determines the activation energy of the corrosion process, increases. Corrosion current density is reduced, which implies that fewer corrosion processes occur. The impedance spectra show that the tested surface has oxide characteristics rather than metallic characteristics, which affects its electro-insulating properties. In a study by RYBALKA et al. (2006), stainless steel with a chromium content of 12.4% exhibited different impedance spectra with a more metallic character. In the presented research, higher chromium content led to a more oxide character. The morphology of oxide coating may have a greater influence on electrochemical processes taking place during the operation of alternating current. It appears that plastic deformation may favor chromium passivation in the presence of air. Such a mechanism is supported by research conducted by NAZAROV et al. (2019). The above effect may lead to an increase in the amount of oxides, and the observed decrease in corrosion potential and polarization current density. The results of the EIS test may prove the homogeneity of the oxide layer on the steel surface. In the tested samples, the homogeneity of the oxide layer probably

increases to a deformation value of 0.12. After exceeding this level, the amount of oxides continues to increase, but a larger number of discontinuities appear, resulting in greater slopes of the impedance spectrum towards the OY axis (imaginary impedance). This effect may be caused by change in the valence of chromium in oxide layers which may be supported by a shift of potential, a sharper decrease in current density and the slopes of impedance spectra after exceeding a strain of 0.12. In a study by MARIJAN and GOJIC (2002), such an effect was found to be indicative of change in the valence of chromium oxide, but in the present experiment, this effect was caused by forced potential changes. From an electrochemical point of view, an increase in strain can exert a similar effect by decreasing the potential for chromium oxide formation and increasing the thickness of the passive layer, as demonstrated by ZHENG et al. (2018).

References

ALVAREZ K., SATO K., HYUN S.K., NAKAJIMA H. 2008. *Fabrication and properties of Lotus-type porous nickel-free stainless steel for biomedical applications*. Materials Science and Engineering C, 28: 44-50.

BASSIONI G., KORIN A., EL-DIN SALAMA A. 2015. *Stainless Steel as a Source of Potential Hazard due to Metal Leaching into Beverages*. International Journal of Electrochemical Science, 10: 3792–3802.

BERNSTEIN I.M. 1977. *Handbook of stainless steels*. McGraw-Hill, New York.

EN 10088-1:2014. *Stale odporne na korozję*. Część 1. *Wykaz stali odpornych na korozję*.

FREIREA L., CARMEZIMA M.J., FERREIRAA M.G.S., MONTEMOR M.F. 2011. *The electrochemical behavior of stainless steel AISI 304 in alkaline solutions with different pH in the presence of chloride*. Electrochimica Acta, 56: 5280–5289.

KUŁAKOWSKI M., ROKOSZ K. 2017. *Stopowe stale austenityczne, ferrytyczne i duplex używane w transporcie*. Autobusy, 7-8: 357–362.

MARIJAN D., GOJIC M. 2002. *Electrochemical study of the chromium electrode behaviour in borate buffer solution*. Journal of Applied Electrochemistry, 32: 1341–1346.

NAZAROV A., VIVIER V., VUCKO F., THIERRY D. 2019. *Effect of Tensile Stress on the Passivity Breakdown and Repassivation of AISI 304 Stainless Steel: A Scanning Kelvin Probe and Scanning Electrochemical Microscopy Study*. Journal of The Electrochemical Society, 166: C3207-C3219.

PN-EN ISO 6892-1. *Metale. Próba rozciągania*. Część 1. *Metoda badania w temperaturze pokojowej*.

RUTKOWSKA-GORCZYCA M., PODREZ-RADZISZEWSKA M., KAJTOCH J. 2009. *Corrosion resistance and microstructure of steel AISI 316L*. Metallurgy and Foundry Engineering, 35: 35–43.

RYAN G., PANDIT A., APATSIDIS D.P. 2006. *Fabrication methods of porous metals for use in orthopaedic applications*. Biomaterials, 27: 2651-2670.

RYBALKA K.V., BEKETAEVA L.A., DAVYDOV A.D. 2006. *Electrochemical behavior of stainless steel in aerated NaCl solutions by electrochemical impedance and rotating disk electrode methods*. Russian Journal of Electrochemistry, 42: 370–374.

SANTONEN T., STOCKMANN-JUVALA H., ZITTING A. 2010. *Review on toxicity of stainless steel*. Finnish Institute of Occupational Health, Helsinki.

Stress Corrosion Cracking in Light Water Reactors: Good Practices and Lessons Learned. 2011. International Atomic Energy Agency, Vienna.

TIAMIYU A.A., EDUOK U., SZPUNAR J.A., ODESHI A.G. 2019. *Corrosion behavior of metastable AISI 321 austenitic stainless steel: Investigating the effect of grain size and prior plastic deformation on its degradation pattern in saline media*. Scientific Reports, 9: 1–18.

VENKATRAMAN M., PAVITRA K., JANA V., KACHWALA T. 2013. *Manufacturing and critical applications of stainless steel – An Overview*. Advanced Materials Research, 794: 163–173.

WCIŚLIK W., KOSSAKOWSKI P., SOKOŁOWSKI P. 2017. *Stainless steel in building structures – advantages and examples of application*. Structure and Enviroment, 3: 191–198.

ZHENG M., SHUAI M., YU J. 2018. *Influence of deformation on electrochemical properties of Q235 steel*. Koroze a ochrana materiálu, 62(3): 108–114.